

See discussions, stats, and author profiles for this publication at: <https://www.researchgate.net/publication/231713015>

# Control of Catalytic Reactions at the Surface of a Metal Oxide Nanowire by Manipulating Electron Density Inside It

ARTICLE *in* NANO LETTERS · FEBRUARY 2004

Impact Factor: 13.59 · DOI: 10.1021/nl034968f

---

CITATIONS

177

---

READS

99

## 5 AUTHORS, INCLUDING:



[Andrei Kolmakov](#)

National Institute of Standards and Technolo...

132 PUBLICATIONS 4,810 CITATIONS

SEE PROFILE



[Steeve Chretien](#)

University of California, Santa Barbara

38 PUBLICATIONS 1,125 CITATIONS

SEE PROFILE



[Horia Metiu](#)

University of California, Santa Barbara

408 PUBLICATIONS 13,580 CITATIONS

SEE PROFILE

# Control of Catalytic Reactions at the Surface of a Metal Oxide Nanowire by Manipulating Electron Density Inside It

Y. Zhang,<sup>†</sup> A. Kolmakov,<sup>\*,†</sup> S. Chretien,<sup>†</sup> H. Metiu,<sup>‡</sup> and M. Moskovits<sup>†</sup>

*Department of Chemistry and Biochemistry and Department of Physics,  
University of California at Santa Barbara, Santa Barbara, California 93103-9510*

*Received October 31, 2003; Revised Manuscript Received January 13, 2004*

## ABSTRACT

We show that the rates and extent of oxidation and reduction reactions taking place at the surface of a SnO<sub>2</sub> nanowire, configured as a field-effect transistor, can be modified by changing the electron density in the wire with a gate voltage.

Oxygen vacancies on many oxide surfaces (e.g., TiO<sub>2</sub>, SnO<sub>2</sub>, etc.) are electrically and chemically active. When vacancies are created, the electrons left behind are localized in states whose energies lie close to the conduction band and function as n-type donors.<sup>1</sup> As a result, the vacancy creation increases the conductivity of the oxide, often significantly. Furthermore, atoms or molecules interacting with the oxide surface tend to bind at the oxygen vacancy sites.<sup>1–3</sup> If the adsorbed molecules are charge acceptors (such as oxygen), then they use the electrons localized at the vacancy sites to make the chemical bond to the surface. As a result, the adsorption of an electron acceptor lowers the conductivity of the n-type oxide. Molecules that react with surface oxygen and remove it create shallow donor states and increase the conductivity. Many solid-state gas sensors make use of this property.<sup>4–7</sup>

Quasi-1D metal oxide nanowires are, in principle, able to improve the performance of chemical sensors significantly and can contribute to a fundamental understanding of these phenomena because they are highly sensitive and tunable electrical transducers of the chemical processes occurring on their surfaces.<sup>8–12</sup>

Experimental observations, supported by calculations, suggest that the availability of electrons at the vacancy site affects the chemical activity of the oxide surface.<sup>1,13,14</sup> The influence of an electrostatic field (and the concomitant change in the near-surface electron density) on adsorption and catalysis occurring on macroscopic semiconductor surfaces was predicted and experimentally verified long ago.<sup>15–19</sup> This subject was revisited in connection with the development of FET-based gas sensors.<sup>20–23</sup> The latter property was inferred from the field dependence of the work function (or

channel conductance) change upon the adsorption of a molecule to an oxide surface configured as a field-effect transistor (FET) with a chemically active gate.

Quasi-1D metal oxide nanowires with diameters in the range of 10–100 nm have attractive properties such as a large surface-to-volume ratio, a radius comparable to the Debye length, and a small total number of electrons ( $10^3$ – $10^5$   $\mu\text{m}^{-1}$  at moderate doping levels). These characteristics make them ideal objects for studying and exploiting the interplay between electron density and surface properties. In the present work, we demonstrate that changes in the surface chemistry of an individual nanostructure configured as an FET can be caused by a controlled change in the electron density in the wire. In particular, we present experimental observations suggesting that the rates of oxygen adsorption–desorption and that of the catalytic oxidation of CO, taking place on the surface of a SnO<sub>2</sub> nanowire, along with the specific reaction channel can be changed by varying the electron density inside the nanowire, with the help of a gate potential.

The FET device used in our experiments is an ~60-nm-diameter SnO<sub>2</sub> wire several micrometers long deposited onto a 300-nm-thick SiO<sub>2</sub> film grown thermally on a heavily boron-doped (0.02  $\Omega$  cm) Si substrate (Figure 1). The Si substrate is used as the gate electrode. The source and the drain electrodes are Ti (20 nm)/Au (200 nm) micropads vapor deposited on the ends of the SnO<sub>2</sub> nanowire, chosen to minimize the Schottky barrier at the contacts.

Rutile-SnO<sub>2</sub> nanowires with average crystalline domains of  $\sim 10^2$ – $10^3$  nm were fabricated by an electrochemical method (described elsewhere<sup>24</sup>) that makes  $\beta$ -Sn nanowires inside porous alumina templates. After being extracted from the alumina matrix, the nanowires were topotactically oxidized to SnO<sub>2</sub> by gradual annealing in air for several

\* Corresponding author. E-mail: akolmakov@chem.ucsb.edu.

<sup>†</sup> Department of Chemistry and Biochemistry.

<sup>‡</sup> Department of Physics.

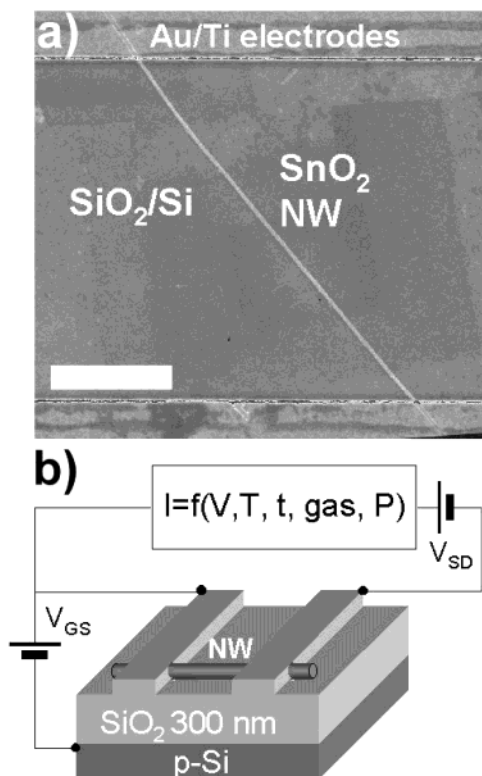


**Figure 1.** (a) SEM image of a  $\text{SnO}_2$  nanowire deposited on a  $\text{SiO}_2/\text{Si}$  substrate, outfitted with Au/Ti electrodes. The white bar is  $1\ \mu\text{m}$  long. (b) Schematic of the nanowire FET.

hours.<sup>25</sup> The use of template synthesis for this study was not a random choice. This synthetic method is capable of producing large arrays of free-standing nanowires that offer attractive design possibilities for fabricating massively parallel sensing and catalytic devices.<sup>12</sup> Conductance measurements were carried out on several individual nanowires, fabricated in different runs, under varying flowing ambient gases and gas mixtures. To elucidate the role of crystallinity in the observed effect, the same studies were performed on highly crystalline vapor-grown nanowires and nanobelts. They exhibited the same qualitative characteristics, indicating that the observed results were robust properties of the nanowires and the devices fabricated from them and were not particularly sensitive to the degree of crystallinity, the specific crystal face on which the process occurs, or the domain size. This observation is not surprising under the “flat-band” conditions that prevail in the systems with reduced dimensionality that are used. Under flat-band conditions, the Schottky barriers that formed between grains as the electron density was reduced (or increased) would be small with respect to  $kT$ . Accordingly, “neck contacts” (if any exist) would not affect the conductivity changes brought about by adsorption onto the nanowire. We found, however, that the reproducibility of the measurements depends on the pretreatment history, the ambient relative humidity, and the age of the wire. These instabilities are caused by charged impurity molecules adsorbed on (and/or near) the surface of the nanowire, which induce the parasitic gating of the nanowire.<sup>26</sup> This implies also that not necessarily all the surface of the nanowire, prepared in this way, is chemically

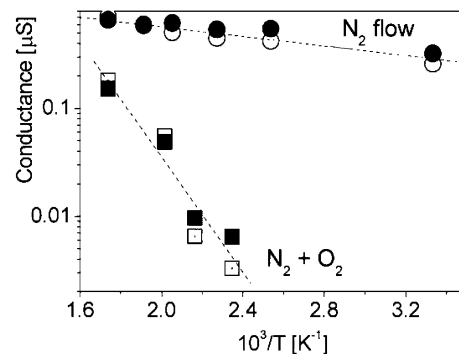


**Figure 2.** Temperature dependence of the conductance of the wire in contact with two different gases. (See text for the gas composition.) Filled and open symbols stand for positive and negative bias  $|V_{\text{DS}}| = 1\ \text{V}$  ( $V_{\text{G}} = 0$ ), respectively.

active. To minimize such effects, the data presented here were obtained for the same nanowire and were acquired within a short period of time. To establish a reference steady-state condition, the wire was pretreated at  $280\text{--}300\ ^\circ\text{C}$  under flowing  $\text{N}_2$  for 2 h before each run.

Under dry nitrogen (100 mL/min) and after several hours of annealing, the nanowire is a fairly good conductor (conductivity  $\sigma = 18\ \Omega^{-1}\text{cm}^{-1}$  at  $300\ ^\circ\text{C}$ ). When the nanowire is exposed to a mixture of  $\text{N}_2$  and  $\text{O}_2$  (100 mL/min of  $\text{N}_2$  and 10 mL/min of  $\text{O}_2$ ), its conductivity drops dramatically to reach a steady state with  $\sigma = 3.8\ \Omega^{-1}\text{cm}^{-1}$  (at  $300\ ^\circ\text{C}$ ). The steady-state conductance, measured at various temperatures  $T$ , was used to determine the activation energy of the carriers. Plots of the natural logarithm of the conductance versus  $1/T$  were fit to straight lines (Figure 2). The measured activation energies under dry nitrogen and nitrogen/oxygen mixtures are 46 and 560 meV, respectively. This implies that there are at least two types of localized electron states in the band gap, near the conduction band edge. The activation energies as well as their ratio differ from nanowire to nanowire, probably because of fluctuations in the nature of electron traps (that depend on the morphological details) and contributions from the small Schottky barriers at contacts.<sup>27</sup>

The change in conductivity caused by contact with these gases is interpreted as follows.<sup>28</sup> When the gas contains nitrogen only (oxygen and water traces can be present at ppm level), oxygen desorbs thermally from the tin oxide surface, creating surface vacancies. The electrons in the shallow donor levels, created by oxygen desorption, are thermally excited into the conduction band. Through this process, increasing the number of vacancies increases the conductivity until a steady state is reached. When oxygen is admitted into the gas flow, the surface adsorbs it at vacancy sites, and the electrons that were localized in the vacancy (and were available for thermal excitation into the conduction band) are tied up into the newly formed Sn–O bonds. The binding energy of these electrons is well below the conduction band, and they can no longer be thermally excited to contribute to the conductivity. Contact with oxygen decreases conductivity.

To explain why the activation energy (of conductivity) increases in the presence of oxygen, we assume that there is a distribution of donor levels near the conduction band and

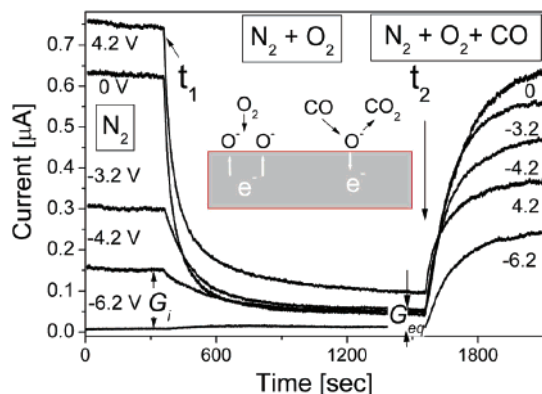


**Figure 3.** Evolution of the conductance of the nanowire exposed to nitrogen (the early, flat part of the curves), to a mixture of nitrogen and oxygen (the decaying part), and to a mixture of oxygen, nitrogen, and CO (the rising part) for different gate voltages.

that the reaction with oxygen depletes the shallow donors more readily. This is consistent with the fact that oxygen adsorption is accompanied by electron transfer from the vacancy to the molecule and the higher-energy electrons are more likely to be donated to oxygen than the lower-energy ones.

We examine next the manner in which the gate voltage affects surface chemistry, which is the main subject of this letter. In Figure 3, we show how the conductivity of a nanowire changes as the ambient (flowing) gas composition is changed from pure nitrogen to a nitrogen/oxygen mixture and then to a  $N_2/O_2/CO$  mixture. Each curve in the graph corresponds to a different gate voltage. All experiments were performed at 300 °C on the same wire under the same conditions. Before each adsorption/desorption experiment, the wire was held under the flux (100 mL/min) of dry nitrogen for about 2 h until a steady-state conductance at a particular gate voltage was reached. This was done to create a steady-state number of oxygen vacancies before we introduce oxygen into the system. We note that each experiment with a new gate voltage starts with different concentration of vacancies at steady state.

When 10 mL/min of oxygen was added to the 100 mL/min  $N_2$  flow (at time  $t_1$  in Figure 3), the source–drain current decreases drastically and eventually reaches a new steady state. At some time  $t_2$  after that, CO is introduced into the gas mixture (100 mL/min  $N_2$ , 10 mL/min  $O_2$ , and 5 mL/min CO). CO reacts with  $SnO_2$  to produce  $CO_2$ , leaving behind oxygen vacancies. This creates new donor states, which cause an increase in conductance. At the same time, oxygen adsorption–desorption takes place, and this also affects the number of vacancies. The overall reaction is the catalytic oxidation of CO to  $CO_2$  at the tin oxide surface.

Figure 3 indicates that the gate voltage influences the extent and rate of surface vacancy annihilation and formation when the surface is exposed to oxygen or to a mixture of oxygen and CO. We analyze first the decaying portion of these curves. If the chemical kinetics were adsorption–desorption of oxygen at the vacancy sites of a single type and if the conductance were proportional to the number of vacancies, then the time decay of the conductance would be

given by the function  $G(t) = G_{eq} + (G_i - G_{eq}) \exp[-kt]$ . Here,  $k$  is the sum of the rate constants for oxygen adsorption and desorption, and  $G_{eq}$  and  $G_i$  are the steady-state and the initial conductance, respectively. The kinetics is pseudo-first order because the flux of oxygen to the surface is so high that is changed very little by adsorption and can be treated as a constant and incorporated into the rate constant. A least-squares fit of the data with this function leads to errors as large as 20%. The kinetics of the descending curves in Figure 3 cannot be accounted for by a model that decays with only one time scale. The latter result is not surprising. The fact that the conductivity has two activation energies hints that we need to consider at least two kinds of adsorption sites. The kinetic scheme that considers two adsorption rates for oxygen (corresponding to two dominating different binding sites) and two rates of vacancy ionization (corresponding to two types of vacancies) gives the following type of equation for the decay of conductivity caused by exposure to oxygen:

$$G(t) = G_{eq} + (G_i - G_{eq} - a) \exp[-k_1 t] + a \exp[-k_2 t] \quad (1)$$

Here  $a$ ,  $k_1$ , and  $k_2$  are fitting parameters. The “rate constants”  $k_1$  and  $k_2$  are complicated combinations of the oxygen adsorption and desorption rate constants for the two kinds of vacancies and of the rate constants for the transition of the electrons from the two localized vacancy states to the conduction band. Similarly,  $a$  is a function of the rate constants and the initial concentration. The oxygen pressure is incorporated into the adsorption rate constant. (It is constant throughout the experiment.) The specific expressions for  $k_1$ ,  $k_2$  and  $a$  depend on the details of the model and will not be discussed here because they involve tedious but elementary chemical kinetics.

The nature of the two states invoked by the kinetic model was not addressed in this study: they could be vacancies containing one or two localized electrons, or there may be a distribution of vacancies (whose properties vary because of differences in their environment) whose behavior can be represented by a two-state model (such as the Anderson model for the heat capacity of glasses). In addition, the real multifaceted oxide surface poses vacancies with different coordination: for example, in-plane or bridging oxygen vacancies at  $SnO_2$  (110), at step edges, or at kink sites. It is a well-documented power and weakness of phenomenological kinetics that it lumps all elementary physical processes into the rate constants and the concentration of the participating species: the microscopic nature of the reaction participants is hard to determine because it manifests itself only through the numerical values of the rate constants.

Equation 1 fits the data rather well (the plot representing the data coincides with that of the fitting function) with the fitting parameters given in Table 1.

We discuss first the reaction of the surface with oxygen. The time constants produced by these fits are plotted as a function of gate potential in Figure 4. As can be seen, the rate constants ( $k_1$  and  $k_2$ ) characterizing this reaction have very different gate dependences:  $k_2$  remains almost independent of gate potential, but  $k_1$  is small at negative gate



**Table 1.** Parameters  $a$ ,  $k_1$ , and  $k_2$  Obtained by Fitting the Data with the Curve Given by Equation 1 for the Decaying<sup>a</sup> and Rising<sup>b</sup> Parts of the Curves.

| $V_g$ [V] | descending part |                                    |                                    | rising part |                                    |                                    |
|-----------|-----------------|------------------------------------|------------------------------------|-------------|------------------------------------|------------------------------------|
|           | $a$             | $k_1$<br>$10^2$ [s <sup>-1</sup> ] | $k_2$<br>$10^2$ [s <sup>-1</sup> ] | $a$         | $k_1$<br>$10^2$ [s <sup>-1</sup> ] | $k_2$<br>$10^2$ [s <sup>-1</sup> ] |
| -4.2      | 0.04            | 0.62                               | 0.21                               | -0.30       | 1.13                               | 0.75                               |
| -3.2      | 0.04            | 0.87                               | 0.22                               | 3.51        | 0.70                               | 0.69                               |
| -2.2      | 0.02            | 0.86                               | 0.18                               | 5.60        | 0.57                               | 0.55                               |
| 0         | 0.16            | 3.00                               | 0.47                               | 0.10        | 0.57                               | 0.20                               |
| 2.2       | 0.17            | 2.87                               | 0.37                               | -0.26       | 3.55                               | 0.56                               |
| 4.2       | 0.19            | 2.45                               | 0.34                               | -0.19       | 4.04                               | 0.68                               |
| 6.2       | 0.21            | 2.64                               | 0.33                               | -0.17       | 4.48                               | 0.65                               |

<sup>a</sup> Oxidation of the surface. <sup>b</sup> Reduction of the surface by CO.

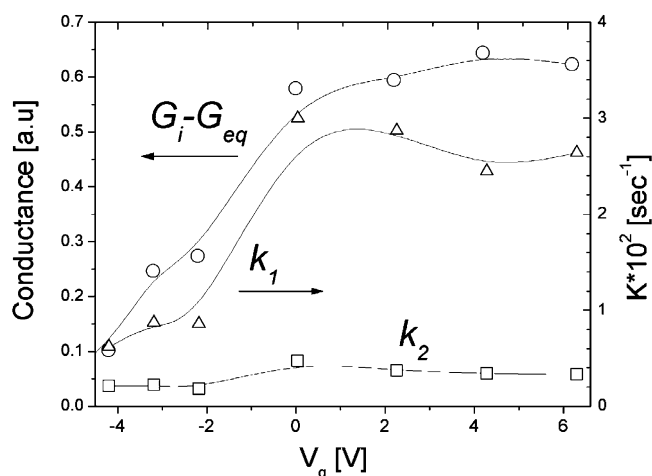


**Figure 4.** Dependence of the rate constants  $k_1$  and  $k_2$  and the extent of reaction for oxygen ionosorption on the gate potential. The lines are drawn to guide the eye.

and increases ca. 5 times at positive gate potential. Little variation of  $k_1$  is seen at positive  $V_g$ . The major changes in kinetics with gate potential are mainly determined by  $k_1$  and take place within a relatively narrow gate voltage interval from 0 to -2.2 V. As we have already stated, our measurements of the activation energy of conductivity show that there are at least two activation energies for the “ionization” of the vacancy electrons to the conduction band and that the introduction of oxygen first consumes the vacancies having smaller activation energies. Because  $k_1$  is larger than  $k_2$ , it controls the short-time scale, which means that it represents the more rapid process. We infer that this is the annihilation of the vacancies having low electron-ionization (to the conduction band) energy. Because  $k_1$  is most strongly affected by the gate, we infer that the gate more strongly affects the weakly bound vacancy electrons.

We note that the relaxation times go as the exponent of the rate expressions; therefore, the effect of the gate voltage on the evolution of the vacancy coverage is more substantial than the effect on the time scale. Indeed, the extent of reaction ( $G_i - G_{eq}$ ), which is a measure of the cumulative oxygen ionosorption in our case, strongly increases with the gate voltage and saturates at high positive  $V_g$ .

The model that we propose for interpreting the descending part of the curves in Figure 3 is based on the long-accepted

idea that oxygen is made reactive by capturing an electron from the oxide and forming a negatively charged intermediate. The rate of this electron capture is controlled by three factors: (1) the number of electrons available at the surface for this donation, (2) the overlap between the orbital of the electron localized at the vacancy site and the empty  $\pi^*$  orbital of oxygen, and (3) the proximity in energy of these two orbitals. This means that the electrons localized in vacancies are the most active.

A negative gate voltage pushes electrons out of the nanowire into the source and drain, diminishing the number of electrons available at the vacancy sites. (The conduction-band electrons and the ones populating the shallow vacancy levels are in thermal equilibrium.) Therefore, by decreasing the number of electrons available for oxygen surface chemistry, electron removal from the nanowire at negative gate potentials lowers the oxidation rate and the extent of oxygen adsorption. This is the trend seen in Figure 4 for the fast adsorption channel  $k_1$  and for ( $G_i - G_{eq}$ ). The gate dependence of the extent of the reaction closely follows the conductance changes  $G_i$  in dry  $N_2$  (not shown here). The latter is in fact the transfer characteristic ( $I_{SD}(V_g)$ ) of the FET device, which is a measure of the initial electron density inside the nanowire.

One would expect that a positive gate voltage would bring electrons into the nanowire, thus increasing its affinity for oxygen. Table 1 and Figure 4 show that this does not happen linearly. Instead, all of the measured parameters exhibit either saturation or even some drop ( $k_1$ ). We have three possible explanations for this: (i) The electron density is saturated inside the nanowire at high positive gate potential. The later effect is often observed in nanowire or carbon nanotube FET devices at high  $|V_g|$  as a saturation of the source-drain current, which becomes limited by nonzero resistance at contacts. (ii) At a certain  $V_g$  value (in our case, close to 0 V), perhaps all of the vacancies are filled with electrons, and increasing the positive gate voltage fills only the conduction bands. The electrons in the conduction band do not overlap well with the  $\pi^*$  orbital of oxygen and therefore do not significantly affect oxygen reactivity. (iii) Another possibility is that the positive gate voltage shifts the donor levels off-resonance with the  $\pi^*$  orbital, thus making electron transfer to the oxygen molecule less likely.

The kinetics leading to the rising part of the curves shown in Figure 3 is more complicated. CO reacts irreversibly with the oxygen at the surface of the nanowire to form  $CO_2$ . Simultaneously, oxygen is adsorbed on the existing vacancies. The net result is an increase in conductance, which indicates that after CO is introduced into the system vacancy creation prevails over vacancy annihilation until a new steady state is reached. The observed CO-induced conductance increase that takes place even at the highest negative gate potentials (bottom curve in Figure 3) where no appreciable oxygen adsorption takes place is likely due to the reaction of CO with lattice oxygen or remaining hydroxyl groups, a process that is not expected to be gate-voltage-dependent.<sup>29</sup> This is an important observation, which demonstrates that the reaction path can be altered by gate potential and

therefore the selectivity of the nanostructure as a sensor or catalyst can be tuned electronically.

Even a simplistic kinetic model that includes CO oxidation and O<sub>2</sub> adsorption and allows for two kinds of vacancies on the surface leads to an expression containing a sum of four decaying exponentials. However, the rising portions of the curves are fit well by the function given by eq 1. This means that of the four exponentials two dominate the behavior of the system. The gate voltage affects CO oxidation differently than it affects oxygen ionosorption. As in the case of oxygen adsorption, the positive voltage has a strong influence on the time scales (predominantly on  $k_1$ ), but the negative voltage has a considerable effect only when it becomes rather large. The results for CO reaction are harder to interpret because CO reacts with surface oxygen (both bridging and in plane oxygen) and it is only indirectly (through the oxidation reaction) affected by the presence of electrons in the conduction band or in the vacancies. It is conceivable that the presence of excess electrons in the wire (positive gate voltage) increases the number of O precursors and accelerates CO oxidation.

Although more work needs to be done to have a complete understanding of the interplay between gate voltage and the chemistry of nanowires, our experiments show that manipulating the number of electrons inside a nanowire affects the chemical reactivity and selectivity of its surface. This opens up the possibility of using solid-state electronics to manipulate the rates and reaction paths of catalytic reactions. When using vapor-grown single-crystal nanowires, the results also illustrate a novel strategy for the fundamental study of catalysis by mesoscopic systems via monitoring the transport properties of the well-defined crystalline nanostructures.

**Acknowledgment.** We thank Alan Heeger, D. Moses, and G. Wang for helpful discussions and for lending us equipment. We are grateful to E. Caine and J.P. Zhang for their help with lithography and HREM. This work was supported by a DURINT grant from AFOSR and made extensive use of the MRL Central Facilities at UCSB supported by the National Science Foundation under award no. DMR96-32716.

## References

- (1) Henrich, V. E.; Cox, P. A. *Surface Science of Metal Oxides*; Cambridge University Press: Cambridge, England, 1996.
- (2) Diebold, U. *Surf. Sci. Rep.* **2003**, *48*, 53.
- (3) Göpel, W.; Rucker, G.; Feierabend, R. *Phys. Rev. B* **1983**, *28*, 3427.
- (4) Göpel, W. *Microelectron. Eng.* **1996**, *32*, 75.
- (5) Kohl, D. *J. Phys D: Appl. Phys.* **2001**, *34*, R125.
- (6) Moseley, P. T. *Meas. Sci. Technol.* **1997**, *8*, 223.
- (7) Sberveglieri, G. *Sens. Actuators, B* **1995**, *23*, 103.
- (8) Law, M.; Kind, H.; Messer, B.; et al. *Angew. Chem., Int. Ed.* **2002**, *41*, 2405.
- (9) Comini, E.; Faglia, G.; Sberveglieri, G.; et al. *Appl. Phys. Lett.* **2002**, *81*, 1869.
- (10) Arnold, M. S.; Avouris, P.; Pan, Z. W.; Wang, Z. L. *J. Phys. Chem. B* **2003**, *107*, 659.
- (11) Han, S.; Jin, W.; Tang, T.; et al. *J. Mater. Res.* **2003**, *18*, 245.
- (12) Kolmakov, A.; Zhang, Y.; Cheng, G.; et al. *Adv. Mater.* **2003**, *15*, 997.
- (13) Oviedo, J.; Gillan, M. J. *Surf. Sci.* **2001**, *490*, 221.
- (14) Göpel, W.; Hesse, J.; Zemel, J. N. *Sensors: A Comprehensive Survey*; VCH: Weinheim, Germany, 1989).
- (15) Keier, N. P.; Mikheeva, E. P.; Usoltsev, L. G. *Dokl. Akad. Nauk SSSR* **1968**, *182*, 130.
- (16) Hoenig, S. A.; Lane, J. R. *Surf. Sci.* **1968**, *11*, 163.
- (17) Devyatov, V. G.; Mikheeva, E. P.; Keier, N. P. *React. Kinet. Catal. Lett.* **1978**, *9*, 199.
- (18) Usoltsev, L. M.; Mikheeva, E. P.; Keier, N. P. *Kinet. Catal.* **1979**, *20*, 128.
- (19) Wolkenstein, T. *Electronic Processes on Semiconductor Surfaces during Chemisorption*; Consultants Bureau: New York, 1991.
- (20) Kunishima, Y. N.; Miyayama, M.; Yanagida, H. *J. Electrochem. Soc.* **1996**, *143*, 1334.
- (21) Hellmich, W.; Müller, G.; Bosch-Von Braunmühl, C.; et al. *Sens. Actuators, B* **1997**, *43*, 132.
- (22) Bogner, M.; Fuchs, A.; Scharnagl, K.; et al. *Appl. Phys. Lett.* **1998**, *73*, 2524.
- (23) Storm, U.; Bartels, O.; Binder, J. *Sens. Actuators, B* **2001**, *77*, 529.
- (24) Moskovits, M.; Routkevitch, D.; Ryan, L.; et al. *Abstr. Pap. - Am. Chem. Soc.* **1995**, *210*, 70.
- (25) Kolmakov, A.; Zhang, Y.; Moskovits, M. *Nano Lett.* **2003**, *3*, 1125.
- (26) Kim, W.; Javey, A.; Vermesh, O.; Wang, Q.; Li, Y.; Dai, H. *Nano Lett.* **2003**, *3*, 193.
- (27) Derycke, V.; Martel, R.; Appenzeller, J.; et al. *Appl. Phys. Lett.* **2002**, *80*, 2773.
- (28) Barsan, N.; Weimar, U. *J. Electroceram.* **2001**, *7*, 143.
- (29) Safonova, O. B. I.; Fabrichnyi, P.; Rumyantseva, M.; Gaskov, A. J. *Mater. Chem.* **2002**, *12*, 11.

NL034968F